proposed antenna are 4.84, 1.96, 8.16, and 3.49 dB at 3.4, 6.8, 9.3, and 10.2 GHz, separately.

4 | CONCLUSION

In this article, an SIW cavity backed equilateral triangle slot antenna is presented. It has multiband characteristic. The position of the feeding point is optimized to excite higher modes. Both of theoretical analysis and simulation are carried out to reveal the working mechanism of TM_{10}, TM_{22}, TM_{12}, and TM_{33}. It is convenient to adjust the resonance frequency by changing the side length of inner equilateral triangular. The measured results have good agreement with simulations.

ACKNOWLEDGMENTS

This work is supported in part by the Natural Science Foundation of China under Grant 61401106 and in part by the Youth Foundation of Guangdong University of Technology 15ZK0038.

ORCID

Yanjie Wu http://orcid.org/0000-0003-0179-7077
Jianfeng Li http://orcid.org/0000-0003-4271-7774

REFERENCES

[1] Deslandes D, Wu K. Single-substrate integration technique of planar circuits and waveguide filters. *IEEE Trans Microwave Theory Tech.* 2003;51(2):593–596.

[2] Xu F, Wu K. Guided-wave and leakage characteristics of substrate integrated waveguide. *IEEE Trans Microwave Theory Tech.* 2005;53(1):66–73.

[3] Li Y, Luk K. A multibeam end-fire magnetoelectric dipole antenna array for millimeter-wave applications. *IEEE Trans Antennas Propag.* 2016;64(7):2894–2904.

[4] Qu S, Ng KB, Chan CH. Waveguide fed broadband millimeter wave short backfire antenna. *IEEE Trans Antennas Propag.* 2013;61(4):1697–1703.

[5] Winkle S, Hong A, Bozzi WM, Wu K. Polarization rotating frequency selective surface based on substrate integrated waveguide technology. *IEEE Trans Antennas Propag.* 2010;58(4):1202–1213.

[6] Liu Y, Shi D, Zhang S, Gao Y. Multiband antenna for satellite navigation system. *IEEE Antennas Wireless Propag Lett.* 2016;15:1329–1332.

[7] Cao YF, Cheung SW, Yuk TI. A multiband slot antenna for GPS/WiMAX/WLAN systems. *IEEE Trans. Antennas Propag.* 2015;63(3):952–958.

[8] CheongWu P, Choi KW, Tam K. Yagi-Uda antenna for multiband radar applications. *IEEE Antennas Wireless Propag Lett.* 2014;13:1065–1068.

[9] Liang Z, Liu J, Li Y, Long Y. A dual-frequency broad-band design of coupled-fed stacked microstrip monopolar patch antenna for WLAN applications. *IEEE Antennas Wireless Propag Lett.* 2016;15:1289–1292.

[10] Zhang T, Hong W, Zhang Y, Wu K. Design and analysis of SIW cavity backed dual-band antennas with a dual-mode triangular-ring slot. *IEEE Trans Antennas Propag* 2014;62(10):5007–5016.

[11] Guan D, Qian Z, Cao W, Ji L, Zhang Y. Compact SIW annular slot antenna with multiband multimode characteristics. *IEEE Trans Antennas Propag.* 2015;63(12):5918–5922.

[12] Han Q, Yang F, Long R, Zhou L, Yan F. Single-fed low-profile high-gain circularly polarized slotted cavity antenna using a high-order mode. *IEEE Antennas Wireless Propag Lett.* 2016;15:110–113.

[13] Helszajn J, James DS. Planar triangular resonators with magnetic walls. *IEEE Trans Microwave Theory Tech.* 1978;26(2):95–100.

How to cite this article: Wu Y, Zhang B, Ding K, Li J, Wu D, Wang K. A design of equilateral triangular ring SIW cavity-backed slot antenna for multiband applications. *Microw Opt Technol Lett.* 2018;60:1193–1199. https://doi.org/10.1002/mop.31137

Received: 25 September 2017

DOI: 10.1002/mop.31136

An analysis of a DGS-inserted stub resonator and its application to an optimum BSF

Imseob Shin[1] | Sangyeol Oh[2] | Changwon Lee[1] | Koohyung Kwon[1] | Young-Sik Kim[2]

[1] Agency for Defense Development, Seoul, 0570, South Korea

[2] Korea University, Seoul, 02841, South Korea

Correspondence
Imseob Shin, Agency for Defense Development, Seoul, 0570, South Korea.
Email: tibab96@gmail.com
Or
Young-Sik Kim, Korea University, Seoul, 02841, South Korea.
Email: yskim@korea.ac.kr

Abstract

A novel defected ground structure (DGS)-inserted stub (DIS) resonator is proposed. The proposed DIS resonator features a typical dumbbell-shaped DGS inserted into an conventional open-circuited stub (OCS) resonator, and it is modeled by a series LC resonator. The inserted DGS can

suppress a harmonic and extend an upper passband. Therefore, the proposed DIS resonator to generate a resonance at 2.0 GHz keeps the upper passband up to 8.0 GHz or higher, while the OCS resonator with the same resonance gives rise to the harmonic at 5.78 GHz. These properties are investigated through EM simulation. Moreover, in order to verify the applicability of the proposed DIS resonator to microwave filters, two optimum bandstop filters (BSFs) with the same stopband at 2.0 GHz using the proposed DIS and OCS resonators are fabricated and measured, respectively. Compared to the optimum BSF using the OCS resonator, the optimum BSF using the proposed DIS resonator shows two notable improvements: a 50% increase in the upper passband and a 15% reduction in the size.

KEYWORDS

bandstop filter (BSF), defected ground structure (DGS), electromagnetic bandgap (EBG), stub resonator

1 | INTRODUCTION

The forbidden bandgap structures such as defected ground structures (DGSs) and electromagnetic bandgap (EBG) structures have been widely investigated in order to improve performances of various microwave components.[1–6] In particular, various DGSs have been proposed to suppress unnecessary passbands and widen stopbands.[1–5]

In this article, a novel DGS-inserted stub (DIS) resonator is proposed. The proposed DIS resonator features a typical dumbbell-shaped DGS that is inserted into a conventional open-circuited stub (OCS) resonator. While many DGSs are mostly used to remove unwanted passbands and widen stopbands, the DGS inserted in the OCS resonator is used to suppress the harmonic and extend the upper passband. Moreover, as a DGS can be substituted for an inductor,[1,5] the proposed DIS resonator requires a shorter physical length, which helps in compact designs. The DIS and OCS resonators with the same resonance at 2.0 GHz are designed and investigated through EM simulation. The OCS resonator gives rise to the harmonic at 5.78 GHz. However, the DIS resonator maintains the upper passband up to 8.0 GHz or higher, without generating any harmonic. The stub length of the DIS resonator is 33% shorter than that of the OCS resonator. Finally, in order to verify the applicability of the proposed DIS resonator to microwave filters, two optimum BSFs with the same stopband at 2.0 GHz are designed, fabricated, and measured. One is based on the proposed DIS resonator and the other on the OCS resonator. Compared to the OCS-based optimum BSF, the upper passband of the DIS-based optimum BSF is increased by 50% and its size is reduced by 15%.

2 | CONFIGURATION AND CHARACTERISTICS

Figure 1A shows the configuration of the proposed DIS resonator. The proposed DIR resonator consists of the conventional OCS resonator and the typical dumbbell-shaped DGS that is located under the T-junction. The inset of Figure 1A shows the geometric parameters of the inserted DGS. Figure 1B shows the conventional OCS resonator, which is represented as a shunt-connected series RLC resonator and the resistor is so small that it is generally omitted.

In order to investigate the characteristics of the proposed DIS resonator, the two stub resonators with the same resonance at 2.0 GHz are designed. One is based on the DIS resonator in Figure 1A and the other on the OCS resonator in Figure 1B. The parameter values for the equivalent circuit of

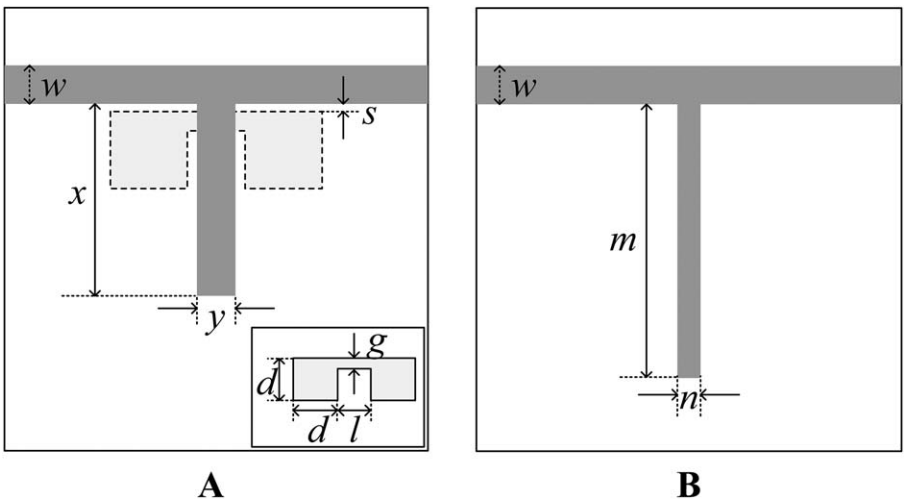

FIGURE 1 Configuration. A, DGS-inserted stub (DIS) resonator. B, Open-circuited stub (OCS) resonator

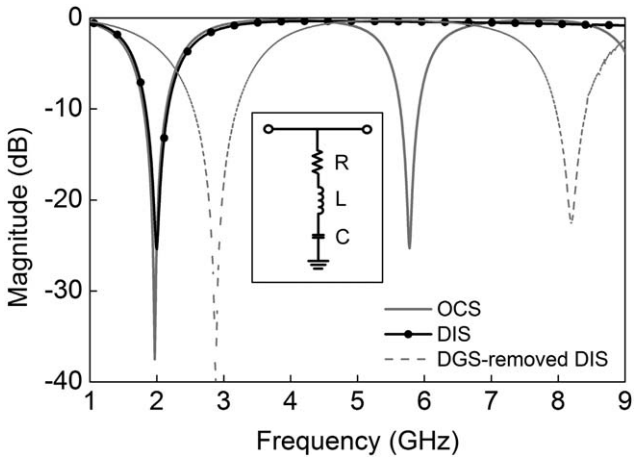

FIGURE 2 Comparison of transmission responses between the DIS and OCS resonators

the OCS resonator are as follows: $L = 3.93$ nH and $C = 1.61$ pF. The design procedure of the DIS resonator is described in the following section. Their dimensions are as follows: $x = 12.1$ mm, $y = 2.2$ mm, $s = 0.5$ mm, $d = 4.0$ mm, $l = 3.5$ mm, $g = 1.5$ mm, $m = 18.25$ mm, and $n = 1.16$ mm. The width (w) of the conductor strip on the substrate is 1.85 mm, corresponding to 50 Ω characteristic impedance. The Rogers RT/Duroid 6006 substrate with a relative dielectric constant of 6.15 and thickness of 1.27 mm is used. All the simulations in this article have been carried out by using ANSYS HFSS.

Figure 2 shows the simulated insertion losses of the DIS and OCS resonators. The DGS-removed DIS resonator, which is an ordinary stub resonator that is obtained by removing the inserted DGS from the DIS resonator, is also simulated, and the results are shown together in Figure 2, for reference. The simulated results of the two stub resonators are almost identical at frequencies below 4.5 GHz, and thus the proposed DIS resonator can be also modeled by the series RLC resonator, which is shown in the inset of Figure 2. However, while the OCS resonator gives rise to the harmonic in the vicinity of 6.0 GHz, the DIS resonator keeps its upper passband up to 8.0 GHz or higher.

Figure 3A shows the simulated insertion and return losses of the DGS resonator, and the inset of Figure 3A shows the configuration of the simulated DGS resonator located under the 50 ohm transmission line. The pattern and size of the DGS resonator is the same with the inserted DGS in the inset of Figure 1A, and the same substrate is also used. The DGS resonator operates as an one-pole BSF with a wide stopband centered at 7.4 GHz. When the DGS resonator is located between the stub resonator and the 50 ohm transmission line, it behaves like a BSF preventing a harmonic signal from going into the stub resonator. As a result, the harmonic signal is reflected back into the load port and the harmonic does not show up. Figure 3B shows the current distribution

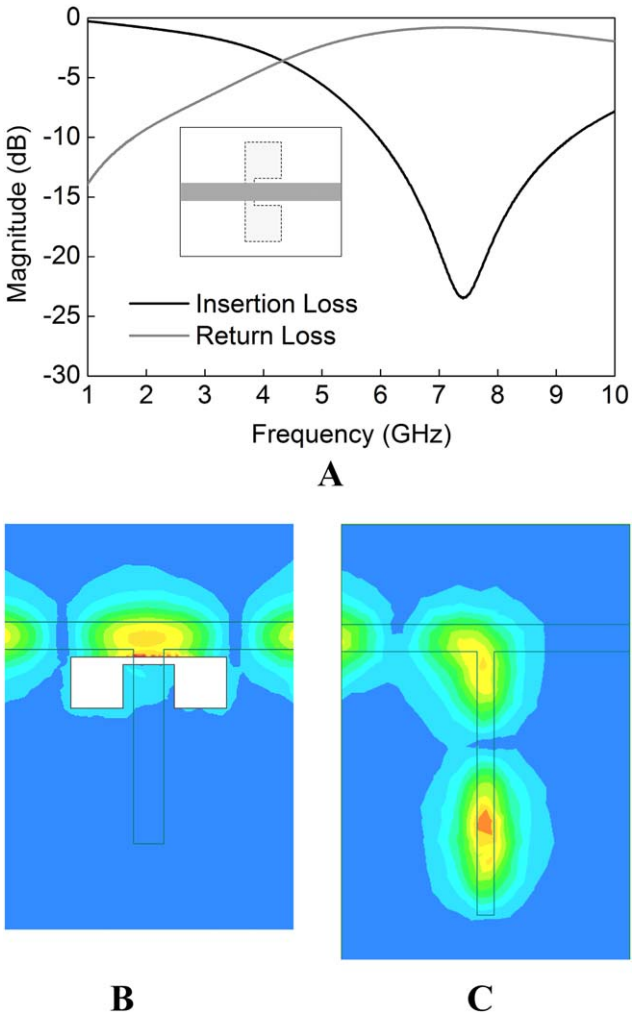

FIGURE 3 A, Simulated results of the DGS resonator. B, Current distribution of the DIS resonator at 6.0 GHz. C, Current distribution of the OCS resonator at 6.0 GHz [Color figure can be viewed at wileyonlinelibrary.com]

at 6.0 GHz on the ground plane of the DIS resonator, which illustrates the results described above. In contrast, Figure 3C shows that the current at 6.0 GHz in the OCS resonator flows into the stub and is reflected back to the source port.

Figure 4 shows the equivalent circuit for the DIS resonator. The DGS is typically modeled by the parallel LC resonator, but it can be substituted for an inductor in a lower

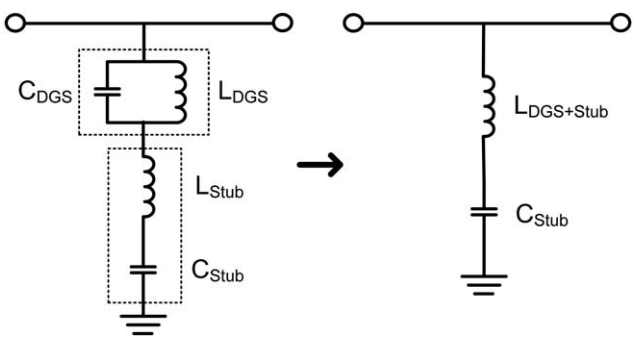

FIGURE 4 Equivalent circuit for the DIS resonator

TABLE 1 Extracted equivalent circuit parameters

Class		Stub length [mm]	L [nH]	C [pF]	f_0 [GHz]
OCS resonator		18.25	3.965	1.646	1.97
DIS resonator	DIS resonator	12.1	4.093	1.547	2.0
	(1) DGS-removed DIS resonator	12.1	2.073	1.451	2.9
	(2) DGS resonator	-	2.753	0.168	7.4
Circuit parameter		-	3.930	1.610	2.0

frequency range than its resonance.[1,5] When the DGS is inserted into the stub resonator, it increases the inductance value of the stub resonator. Consequently, the stub length of the DIS resonator is decreased in proportion to the added inductance value and the DIS resonator is also modeled by the series LC resonator, without change. In Figure 4, the resistor is omitted and the inductor consists of two components: one by the inserted DGS and the other by the stub resonator.

Table 1 shows the circuit parameters of the DIS, OCS, and DGS-removed DIS resonators, which are extracted from the simulated results in Figure 2 using the following equations[6]:

$$R=\frac{Z_0|S_{21}|}{2(1-|S_{21}|)}\Big|_{f=f_0} \quad (1)$$

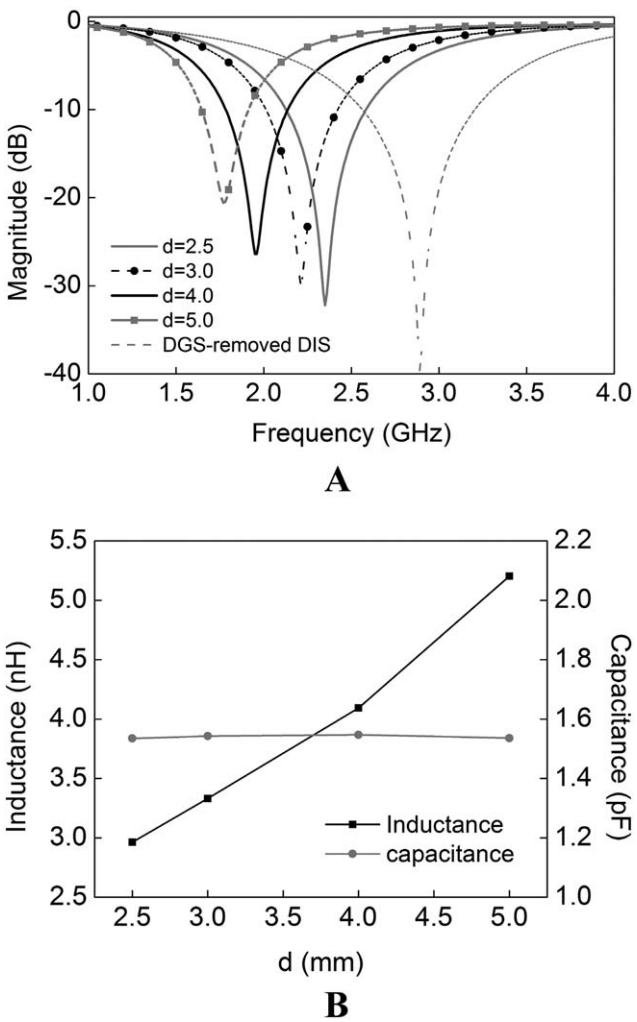

FIGURE 5 A, Simulated results of the proposed DIS resonator for different lattice sizes. B, Extracted circuit parameters

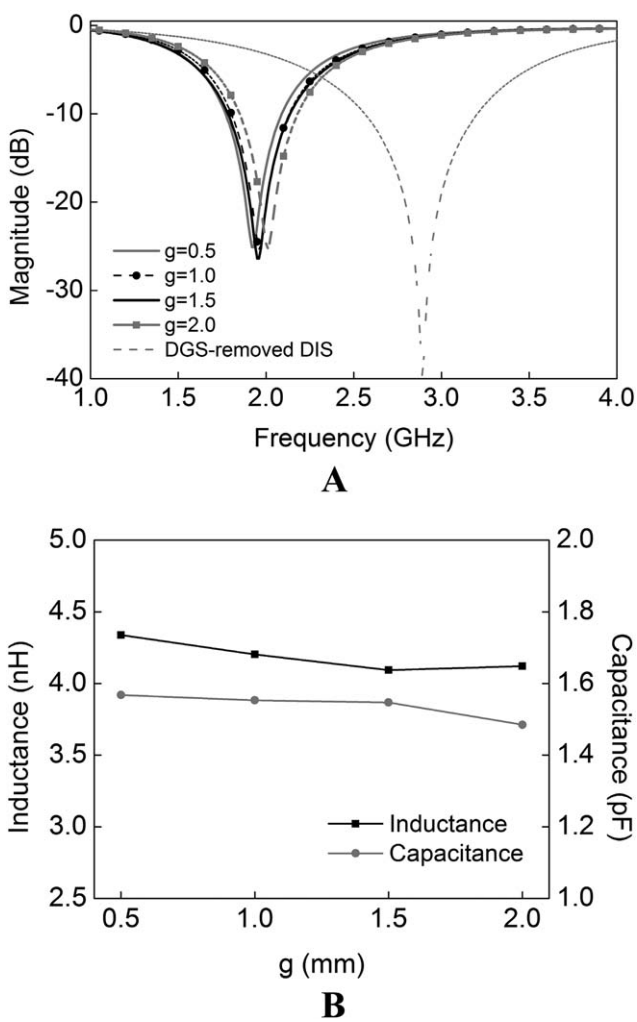

FIGURE 6 A, Simulated results of the proposed DIS resonator for different gaps. B, Extracted circuit parameters

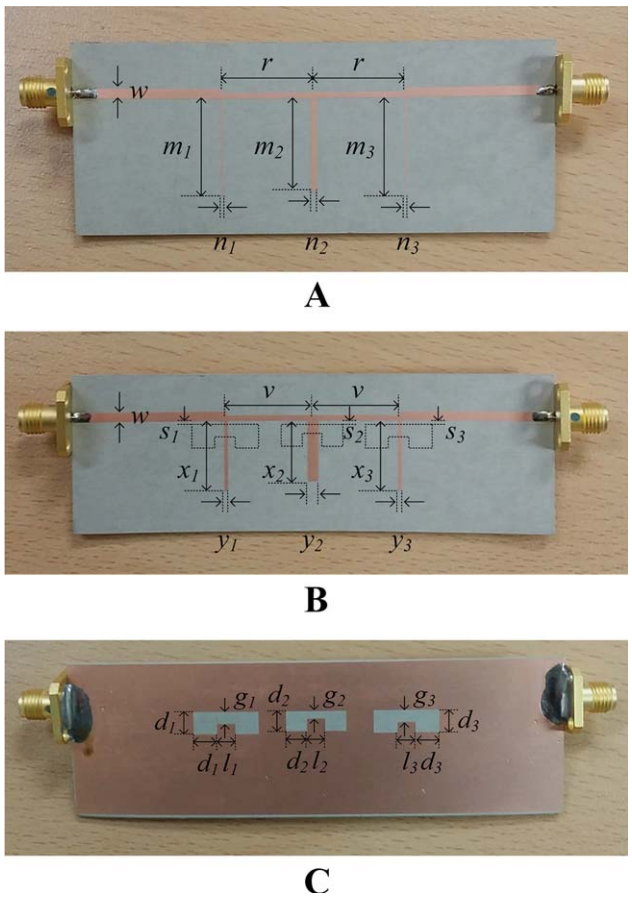

FIGURE 7 Fabrication of optimum BSFs. A, OCS-based optimum BSF. B, DIS-based optimum BSF (top-view). C, DIS-based optimum BSF (bottom-view) [Color figure can be viewed at wileyonlinelibrary.com]

$$L=\frac{\sqrt{0.316^2(2R+Z_0)^2-4R^2}}{11.9\Delta f} \tag{2}$$

$$C=\frac{1}{(2\pi f_0)^2 L} \tag{3}$$

where Z_0 is a characteristic impedance of the transmission line. f_0 is the resonant frequency and Δf is a 10 dB bandwidth. On the other hand, according to the approach proposed by Ref. [1], the circuit parameters for the DGS resonator are extracted from the results in Figure 3A and are also listed in Table 1. From Figure 4 and Table 1, it is shown that when the DGS resonator is inserted into the DGS-removed DIS resonator, approximately 73.5% of the inductance value extracted from the DGS resonator is added to the DGS-removed DIS resonator. Therefore, the stub length of the DIS resonator is reduced by 33.5% compared to that of the OCS resonator. Meanwhile, the inserted DGS increases the capacitance value of the DGS-removed resonator by 6.6%. The current flow changed by the inserted DGS is thought to affect the increase in the capacitance value, which is very small and thus is relatively insignificant.

3 | PARAMETER ANALYSIS

In order to study the effect of the inserted DGS on transmission responses, the proposed DIS resonator is simulated by changing two geometric parameters of the inserted DGS.

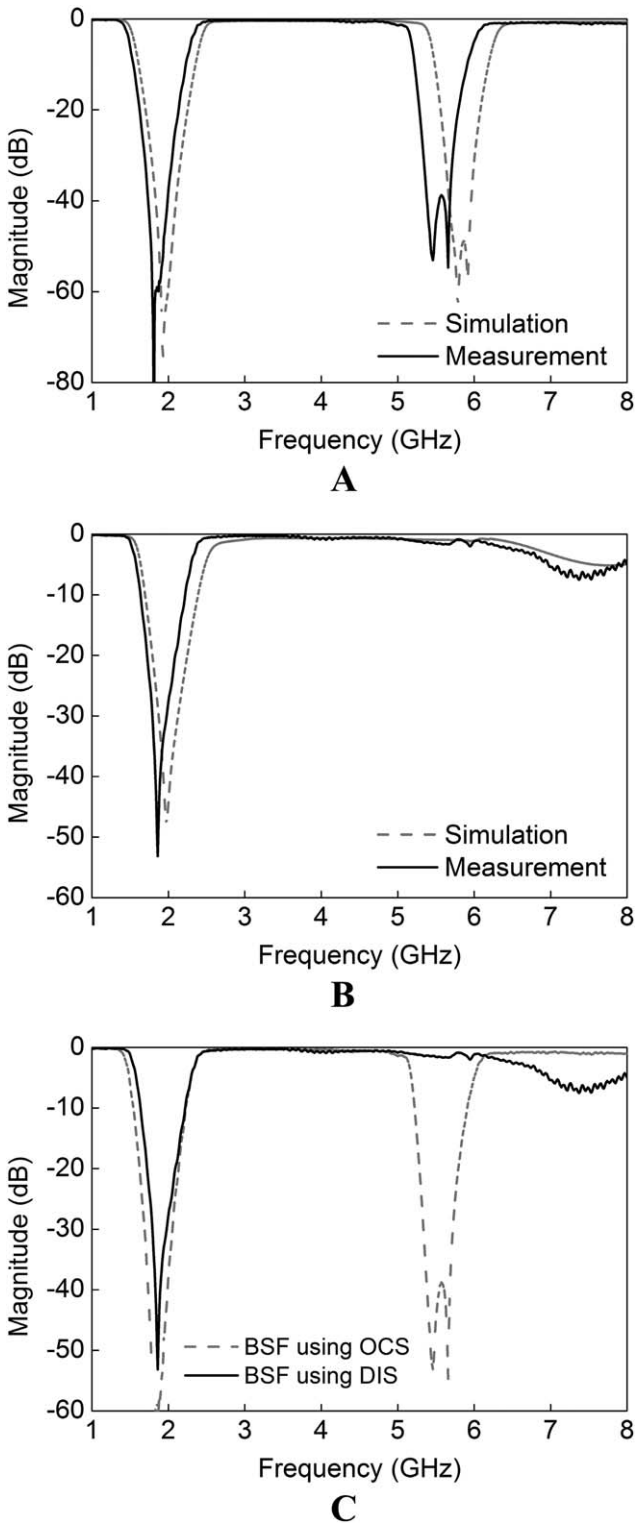

FIGURE 8 Simulated and measured results. A, OCS-based optimum BSF. B, DIS-based optimum BSF. C, Comparison of measured results

Figure 5A shows the transmission responses of the proposed DIS resonators, whose simulations are conducted for four different lattice dimensions. For reference, the responses of the DGS-removed DIS resonator are also shown. The circuit parameters extracted for four lattice sizes are shown in Figure 5B. As the lattice size increases, the effective inductance steeply increases so that the resonant frequency moves to a lower band. On the other hand, the effective capacitance is almost unchanged.

Figure 6A shows the transmission responses of the proposed DIS resonators, which are simulated for four different gap dimensions. The extracted circuit parameters are shown in Figure 6B. The resonant frequency and bandwidth are almost unchanged, which shows that the gap parameter does not affect the resonance as expected in Figure 4. All the parameters in Figures 5B and 6B are also extracted using the three equations mentioned above.

Based on the findings so far, the design procedure of the DIS resonator can be obtained. In case of the OCS and DGS-removed DIS resonator, although the circuit parameters in Table 1 are extracted from EM simulation, the physical dimensions can be simply calculated[7] and are already in Figure 1. First, the DGS-removed DIS resonator with half of the required inductance value can be calculated, and then the DGS resonator can be designed to implement the other half of the inductance value according to Ref. [1]. However, it is noted that about 70% to 75% of the inductance value extracted from the DGS resonator is added. Therefore, all the approximate physical dimensions for the DIS resonator are obtained. Finally, some tuning process through EM simulators is required for accurate dimensions.

4 | BSF WITH EXTENDED UPPER PASSBAND

In order to verify the applicability of the proposed DIS resonator to microwave filters, two 3rd-order optimum BSFs with the same stopband are designed and fabricated.[7] The optimum BSFs have a midband frequency of $f_0 = 2.0$ GHz, ripple constant of 0.1005, and fractional bandwidth of 0.6. One is the conventional optimum BSF based on the OCS resonator, and it is shown in Figure 7A. The dimensions are as follows: $w = 1.85$ mm, $m_1 = m_3 = 19.2$ mm, $m_2 = 18.25$ mm, $n_1 = n_3 = 0.26$ mm, $n_2 = 1.16$ mm, and $r = 18.25$ mm. The other is the proposed optimum BSF based on the DIS resonator, and it is shown in Figure 7B,C. The dimensions are as follows: $w = 1.85$ mm, $s_1 = s_2 = s_3 = 0.5$ mm, $x_1 = x_3 = 14.0$ mm, $x_2 = 13.2$ mm, $y_1 = y_3 = 0.7$ mm, $y_2 = 2.0$ mm, $v = 18.25$ mm, $d_1 = d_3 = 4.5$ mm, $d_2 = 4.0$ mm, $g_1 = g_3 = 2.4$ mm, $g_2 = 1.5$ mm, and $l_1 = l_2 = l_3 = 3.5$ mm. Figure 7B,C show the top and bottom views of the DIS-based optimum BSF, respectively, and the dotted lines in Figure 7B represent the respective DGSs shown in Figure 7C. The difference between the two optimum BSFs is that the OCS resonators are replaced with the DIS ones.

Figure 8A shows the simulated and measured transmission responses of the OCS-based optimum BSF, and Figure 8B shows the results obtained from the DIS-based optimum BSF. The measured results agree with the simulated ones very well except that they are slightly moved downwards. The discrepancy between simulation and measurement is thought to be mainly because of fabrication tolerance. Figure 8C compares the measured results of the two optimum BSFs, which clearly shows that the DIS-based optimum BSF removes the spurious stopband and extends the upper passband. The −3.0 dB upper passband of the DIS-based optimum BSF is maintained up to 6.65 GHz, while that of the OCS-based optimum BSF is terminated at 5.15 GHz. The 1.5 GHz extension of the upper passband is equivalent to the bandwidth increase of about 50%. Moreover, as the stub length is reduced, the DIS-based optimum BSF is about 15.0% smaller than the OCS-based optimum BSF.

5 | CONCLUSION

In this article, the novel DIS resonator is presented, which features the dumbbell-shaped DGS inserted into the general stub resonator. The effects of the inserted DGS on the transmission responses are investigated through EM simulation, and they are as follows: a harmonic suppression, an extension of upper passband, and a reduction of stub length. In addition, the optimum BSF with the extended upper passband is implemented using the proposed DIS resonator. Its improved performances are verified through fabrication and measurement. The proposed DIS resonator is expected to be widely applied wide-band microwave components.

ORCID

Imseob Shin http://orcid.org/0000-0002-6239-4143
Changwon Lee http://orcid.org/0000-0002-8459-2239

REFERENCES

[1] Ahn D, Park J-S, Kim C-S, Kim J, Qian Y, Itoh T. A design of the low-pass filter using the novel microstrip defected ground structure. *IEEE Trans Microwave Theory Tech.* 2001;49(1):86–93.

[2] Lee J-K, Kim Y-S. Ultra-wideband bandpass filter with improved upper stopband performance using defected ground structure. *IEEE Microwave Wireless Compon Lett.* 2010;20(6):316–318.

[3] Sharkawy MAI, Boutejdar A, Galal E. Design of ultra-wide stopband DGS low-pass filter using meander- and multilayer-techniques. *Microwave Opt Technol Lett.* 2013;55(6):1276–1281.

[4] Woo D-J, Lee T-K. Suppression of harmonics in Wilkinson power divider using dual-band rejection by asymmetric DGS. *IEEE Trans Microwave Theory Tech.* 2005;53:2139–2144.

[5] Park J, Kim J-P, Nam S. Design of a novel harmonic-suppressed microstrip low-pass filter. *IEEE Microwave Wireless Components Lett.* 2007;17(6):424–426.

[6] Chang C-, Caloz CC, Itoh T. Analysis of a compact slot resonator in the ground plane for microstrip structures. In: Asia-Pacific Microwave Conference; 2001; 1100–1103.

[7] Hong J, Lancaster M. *Microstrip Filters for RF/Microwave Applications*. New York: Wiley; 2001.

How to cite this article: Shin I, Oh S, Lee C, Kwon K, Kim Y-S. An analysis of a DGS-inserted stub resonator and its application to an optimum BSF. *Microw Opt Technol Lett*. 2018;60:1199–1205. https://doi.org/10.1002/mop.31136

Received: 2 October 2017

DOI: 10.1002/mop.31134

Constant gain modified antipodal vivaldi antenna with rake-like wires operating over 3.1–10.6 GHz

Öznur Küçüksarı[1] | Sibel Çimen[2] | Gonca Çakır[2]

[1] Mechatronics Engineering Department, Kocaeli University, Kocaeli, Umuttepe 41380, Turkey

[2] Electronics and Communication Engineering Department, Kocaeli University, Kocaeli, Umuttepe 41380, Turkey

Correspondence
Öznur Küçüksari, Kocaeli University, Department of Mechatronics Engineering, D Building, Office: D 309, Kocaeli University, Kocaeli, Umuttepe 41380, Turkey.
Email: oznur.kucuksari@kocaeli.edu.tr

Abstract

The main aim of this study is to design an Ultra-Wide Band antenna with an almost constant level of gain over 3.1–10.6 GHz. A modified antipodal Vivaldi antenna with rake-like wires (called MAVARW-III), is designed for this goal. The MAVARW-III has two flared metal arms with rake-like wires printed on a dielectric substrate. Rake-like wires are primarily associated with balancing the gain over the operating bandwidth of the antenna. The proposed MAVARW-III has 7.90 dB minimum gain level over the bandwidth in simulations. The difference between the minimum and maximum value of the gain is <1.55 dB over whole frequency range in simulations. The proposed MAVARW-III is characterized both numerically and experimentally with a good agreement. The given design approach can be extended to relatively larger or smaller MAVARWIIIs to achieve almost constant gain level over desired other frequency bands.

KEYWORDS

antipodal vivaldi antenna, constant gain antenna, flat gain antenna, ultra-wideband antenna

1 | INTRODUCTION

Ultra-wideband technologies over the bandwidth of 3.1–10.6 GHz are common in the wireless communication systems, as well as radar systems. One of the foremost components of these systems is the Ultra-Wide Band (UWB) antenna. One of the desired characteristics for the UWB antennas is having almost constant gain along a given direction over the whole operating range. However, the gain of the lower frequency region of the UWB antennas is inherently lower than the gain of higher frequency region.

Some recent publications have addressed the design of constant gain broadband antennas.[1–6] To the best of our knowledge, having "almost constant gain over 3.1–10.6 GHz" is only demonstrated in the multilayer UWB antenna designs as reported in Refs. [5] and [6]. The Vivaldi antenna and its modified versions[7–11] are common types of the UWB antennas due to its planar geometry, wide operating frequency range, directive radiation pattern, and capability of high gain. Similar to the case of the other UWB antenna types, the Vivaldi antenna and its modified versions have usually lower gain levels at the lower frequencies of the operating bandwidth compared to the higher frequencies.[10,11]

To overcome the constant gain problem especially in the lower frequency region of the UWB, a new modified antipodal single layer Vivaldi antenna is designed. In this study, a modified antipodal Vivaldi antenna with rake-like wires (MAVARW-III) for the purpose of obtaining almost constant gains over 3.1–10.6 GHz as a geometrically simple constant gain UWB antenna is proposed. The presented antenna has 7.90 dB minimum gain level as well as the gain deviation <1.55 dB over 3.1–10.6 GHz in simulations. The MAVARW-III is characterized both numerically and experimentally with a good agreement. The design principles of the suggested UWB antenna topology operating over 3.1–10.6 GHz are anticipated to be useful in the design of the constant gain UWB antennas operating over other bandwidths.